THE ASTROPHYSICAL JOURNAL, 639:L47–L50, 2006 March 10

HAVE WE DETECTED PATCHY REIONIZATION IN QUASAR SPECTRA?

ADAM LIDZ,[1] S. PENG OH,[2] AND STEVEN R. FURLANETTO[3]

Received 2005 December 15; accepted 2006 January 26; published 2006 February 14

ABSTRACT

The Lyα forest at $z \gtrsim 5.5$ shows strong scatter in the mean transmission even when smoothed over extremely large spatial scales, $\gtrsim$50 Mpc h^{-1}. This has been interpreted as a signature of strongly fluctuating radiation fields or patchy reionization. To test this claim, we calculate the scatter arising solely from density fluctuations, assuming a uniform ionizing background, via analytic arguments and simulations. This scatter alone is comparable to that observed. It rises steeply with redshift and is of order unity by $z \sim 6$, even on ~50 Mpc h^{-1} scales. This arises because (1) at $z \sim 6$, transmission spectra, which are sensitive mainly to rare voids, are highly biased (with a linear bias factor $b \geq 4$) tracers of underlying density fluctuations and (2) small-scale transverse modes are aliased to long-wavelength line-of-sight modes. Inferring patchy reionization from quasar spectra is therefore subtle and requires much more detailed modeling. Similarly, we expect density fluctuations alone to produce order unity transmission fluctuations in the $z \sim 3$ He II Lyα forest on the scales over which these measurements are typically made.

Subject headings: cosmology: theory — intergalactic medium — large-scale structure of universe — quasars: absorption lines

Online material: color figures

1. INTRODUCTION

At $z \sim 3$, the structure in the Lyα forest has been shown to arise naturally from density fluctuations in the cosmic web (e.g., Miralda-Escudé et al. 1996). At sufficiently high redshift, however, its structure may instead largely reflect the topology of reionization and/or a strongly fluctuating radiation field. In high-redshift quasar spectra with extended opaque regions, significant gaps of substantial transmission occur (e.g., Becker et al. 2001; White et al. 2003, 2005). This has previously been attributed to a strongly fluctuating UV background, as expected at the tail end of reionization (Wyithe & Loeb 2005; Fan et al. 2005).

Could these transmission gaps simply arise from underdense regions where the neutral hydrogen fraction is lower? The transmission in the $z \sim 6$ quasar spectra differs significantly from sight line to sight line, even when one averages over comoving length scales of ~50–100 Mpc h^{-1}. Since the density variance is small over such large scales, one might naively expect that the reionization of the intergalactic medium (IGM) must be incomplete near $z \sim 6$.

In this Letter, we critically examine this naive intuition. Is rapidly increasing scatter in sight line–to–sight line flux transmission a good diagnostic for patchy reionization (Fan et al. 2002; Lidz et al. 2002; Sokasian et al. 2003; Paschos & Norman 2005)? We find that in fact the fractional scatter in the mean transmissivity of the IGM will be large at high redshift, even for a completely uniform ionizing background. An analogous calculation applies to the case of the He II Lyα forest near $z \sim 3$.

2. THE FLUX POWER SPECTRUM

We adopt the usual "gravitational instability" model of the Lyα forest valid at $z \sim 3$ (e.g., Hui et al. 1997). In particular, we assume an isothermal gas and a uniform photoionization rate Γ and compute whether these assumptions demonstrably break down at $z \sim 6$. Assuming photoionization equilibrium, the Lyα optical depth is $\tau = A\Delta^2$, where $\Delta = \rho/\langle\rho\rangle$, $A \propto (1+z)^{4.5} T^{-0.7}/\Gamma$, and the transmitted flux is $F = e^{-\tau}$. We study the fluctuations in transmitted flux, $\delta_F = (F - \langle F\rangle)/\langle F\rangle$, and its line-of-sight power spectrum, $P_F(k)$. We will also refer to the effective optical depth, $\tau_{\rm eff} = -\ln\langle F\rangle$.

We emphasize that $P_F(k)$ is related to the underlying power spectrum of dark matter density fluctuations $P_\delta(k)$ in a rather complicated way. First, gas pressure smooths the baryons on small scales with respect to the dark matter. Second, a nonlinear transformation maps density into optical depth ($\tau \propto \Delta^2$). Third, one must project from three-dimensional volumes to one-dimensional skewers and incorporate peculiar velocities and thermal broadening. Finally, a second nonlinear transformation maps τ into transmitted flux. These issues are well studied in the context of the $z \sim 3$ Lyα forest (e.g., Croft et al. 2002) but are underappreciated in the reionization literature, which has led to some erroneous conclusions.

2.1. *Analytic Estimates*

We will therefore require numerical simulations to model the flux power spectrum in detail. We can nonetheless anticipate the results with an analytic estimate of the point-to-point flux variance as a function of A and $\tau_{\rm eff}$. We perform this calculation using the Miralda-Escudé et al. (2000) fitting formula for the gas density probability distribution function (PDF):

$$P(\Delta)d\Delta = G\Delta^{-b}\exp\left[-\frac{(\Delta^{-2/3}-C)^2}{8\delta_0^2/9}\right]d\Delta. \quad (1)$$

Here the parameters G and C are fixed by normalizing the PDF to unity, satisfying $\langle\Delta\rangle = 1$. The other parameters are given by $\delta_0 = 7.61/(1+z)$ and $b = 2.5$ at $z = 6$. The first two moments of the (unsmoothed) flux distribution, $\langle F\rangle = \langle e^{-A\Delta^2}\rangle$ and $\langle F^2\rangle = \langle e^{-2A\Delta^2}\rangle$, follow by integrating over $P(\Delta)$.

The method of steepest descents (Songaila & Cowie 2002) yields $\langle F\rangle \sim c\tilde{A}^{1/4}\exp(-d\tilde{A}^{0.4})$ and $\langle F^2\rangle/\langle F\rangle^2 \sim \tilde{c}\tilde{A}^{-1/4}\exp(d\tilde{A}^{0.4})$, where $\tilde{A} = A/25$ and $c = 5.3$, $d = 5.1$, $\tilde{c} = 0.22$, and $\tilde{d} = 3.5$ are constants chosen from full numerical integrations. It fol-

[1] Harvard-Smithsonian Center for Astrophysics, 60 Garden Street, Cambridge, MA 02138.
[2] Department of Physics, University of California, Santa Barbara, CA 93106.
[3] Division of Physics, Mathematics, and Astronomy, California Institute of Technology, Mail Code 130-33, Pasadena, CA 91125.

lows that the fractional point-to-point dispersion will be quite large when A and $\tau_{\rm eff}$ are also large, *even assuming a homogeneous radiation field.* For instance, when $\tau_{\rm eff} \sim 5$ (1), we expect the fractional point-to-point dispersion to be $\sigma_F/\langle F\rangle \sim 4$ (0.8). When $\langle F\rangle \ll 1$, the dominance of rare voids for transmission drastically increases the point-to-point variance.

2.2. *Numerical Simulations*

To be more accurate, and to consider transmission fluctuations smoothed over large scales as well as to include peculiar velocities and thermal broadening, we calculate the flux power spectrum numerically. We use an HPM (Gnedin & Hui 1998) simulation with 2×512^3 particles and 512^3 mesh points in a 40 h^{-1} Mpc box.[4] The simulation implements HPM within the parallel N-body code, MC^2 (see Heitmann et al. 2005 and Lidz et al. 2006).

We take the baryon density and peculiar velocity fields from the simulation and extract artificial spectra in the usual manner (see, e.g., Hui et al. 1997). Specifically, we adjust A to match $\langle F\rangle = 0.20$, 0.13, 0.06, and 0.01 at $z = 4.9$, 5.3, 5.7, and 6.0, respectively. These values are only slightly larger than the measurements of Becker et al. (2001), White et al. (2003), and Fan et al. (2005).

In order to consider large-scale transmission fluctuations, we extrapolate to scales larger than the simulation box by assuming that the flux and one-dimensional linear matter power spectra differ only in normalization and not in shape on large scales (linear biasing e.g., Scherrer & Weinberg 1998), although we show in § 3 that the bias *increases sharply with increasing redshift*. We normalize the extrapolation to the simulated flux power spectrum at $k \sim k_f/2$, where k_f is the fundamental mode of the box. The flux power spectrum is relatively flat on these scales, so our results are not terribly sensitive to the details of this extrapolation.[5]

Figure 1 shows the simulated flux power spectrum. Its amplitude clearly increases rapidly with redshift, even though the density fluctuations decline. In particular, fractional fluctuations are of order unity at $L \sim 35$ Mpc h^{-1} at $z \sim 6$, *even for a uniform radiation field*. Thus, it may be difficult to detect patchy reionization via transmission fluctuations (see § 3).

Figure 1 also shows that the flux power spectrum is quite flat on large scales, because absorption spectra provide only a one-dimensional skewer through the IGM. Ignoring redshift space distortions,

$$P_{\rm 1D}(k_\parallel) = \int_{k_\parallel}^{\infty} \frac{dk}{2\pi}\, kP_{\rm 3D}(k) \qquad (2)$$

at line-of-sight wavenumber $k_\parallel$. Thus, the one-dimensional power spectrum falls off much more slowly toward large scales than the three-dimensional power spectrum does. This aliasing process, whereby transverse short-wavelength modes alias power to long-wavelength line-of-sight modes, is well known in pencil-beam galaxy surveys (Kaiser & Peacock 1991). To illustrate this quantitatively, we consider the amplitude of three-dimensional fluctuations in the nonlinear baryon-density field, $\Delta_b^2(k) = k^3P_b(k)/(2\pi^2)$, where we approximate $P_b(k) = e^{-2k^2/k_f^2}P_\delta(k)$ with $k_f = 20\ h$ Mpc^{-1} (Gnedin & Hui 1998), and use fitting formulae from Peacock & Dodds (1996) and Eisenstein & Hu (1999) for $P_\delta(k)$. The associated variance of one-dimensional baryonic fluctuations, $\Delta^2_{{\rm 1D},\,b}(k_\parallel) = k_\parallel P_{{\rm 1D},\,b}(k_\parallel)/\pi$, at $|\boldsymbol{k}| = k_\parallel$, is ~5.5–10.6 times larger than $\Delta_b^2(k)$ for modes with wavelengths $L \sim 50$–100 Mpc h^{-1}. Fluctuations averaged over a skewer of a given length are much larger than fluctuations averaged over an entire sphere of comparable size.

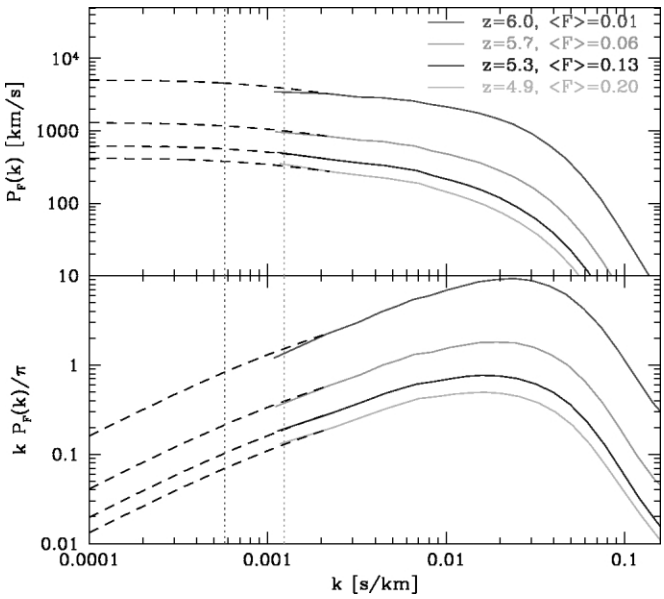

FIG. 1.—Flux power spectrum as a function of scale at various redshifts normalized to the mean flux level $\langle F\rangle$ shown. The dashed lines extrapolate the simulation results to larger scales (see text). The light gray and dark gray dotted lines correspond, respectively, to $L = 35$ and 75 Mpc h^{-1} at $z = 6$. Notice that $kP_F(k)$ decreases only slowly toward large scales because of aliasing. At $z \sim 6$, the fluctuations are of order unity even on scales close to ~50 Mpc h^{-1}. [*See the electronic edition of the Journal for a color version of this figure.*]

3. THE SIGHT LINE–TO–SIGHT LINE SCATTER

The fractional sight line–to–sight line variance in the transmission smoothed on scale L is (Lidz et al. 2002)

$$\frac{\sigma^2_{\langle F\rangle}}{\langle F\rangle^2} = 2\int_0^\infty \frac{dk}{2\pi}\, P_F(k)\left[\frac{\sin\,(kL/2)}{(kL/2)}\right]^2. \qquad (3)$$

Shot noise is negligible for significant stretches of spectrum with at least a moderate signal-to-noise ratio (Lidz et al. 2002). Note that $\sigma_{\tau_{\rm eff}} = \sigma_{\langle F\rangle}/\langle F\rangle$ for small fluctuations.

Figure 2 shows that, like $P_F(k)$ (Fig. 1), the fractional dispersion increases rapidly with decreasing transmission and falls off only slowly as $L \to \infty$.[6] For $z \sim 6$ and $\langle F\rangle = 0.01$ ($\tau_{\rm eff} = 4.6$), $\sigma_{\langle F\rangle}/\langle F\rangle \sim 1$ over ~35 Mpc h^{-1}, even though density fluctuations are small on these scales. Transmission fluctuations are amplified relative to density fluctuations by a bias factor $b = (\sigma_{\langle F\rangle}/\langle F\rangle)/\sigma_{\rho,\,\rm 1D} \sim 4$ when $\tau_{\rm eff} \sim 4$–5 (and increasing at higher $\tau_{\rm eff}$). Thus, although the flux and density power spectra have the same shape on large scales, one *cannot* simply assume that $\sigma_{\langle F\rangle}/\langle F\rangle \sim \sigma_{\rho,\,\rm 1D}$ (as in Wyithe & Loeb 2005 and Fan et al. 2005).

Note that reionization simulations have usually been performed in boxes of $L_{\rm box} \leq 10$ Mpc h^{-1} (see, e.g., Gnedin 2000, Sokasian et al. 2003, and Paschos & Norman 2005, although see Kohler et al. 2005 and Iliev et al. 2005). Mock spectra are normally generated by wrapping long lines of sight around these

[4] We assume a ΛCDM cosmology with $(\sigma_8, h, \Omega_b h^2, \Omega_m, \Omega_\Lambda) = (0.84, 0.7, 0.02, 0.3, 0.7)$.

[5] For instance, extrapolation with a power law changes the transmission dispersion, eq. (3), by only ~20%.

[6] In this regime, $P_F(k)$ is nearly white noise, and $\sigma^2_{\langle F\rangle}/\langle F\rangle^2 \propto L^{-1}$.

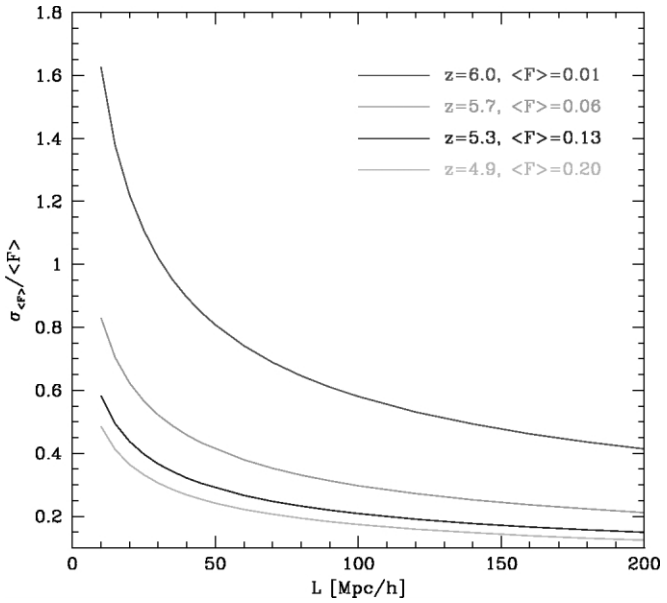

FIG. 2.—Sight line–to–sight line scatter in the mean transmission as a function of scale at several redshifts. The fractional scatter increases rapidly with decreasing transmission and dies off only slowly toward large scales. [*See the electronic edition of the Journal for a color version of this figure.*]

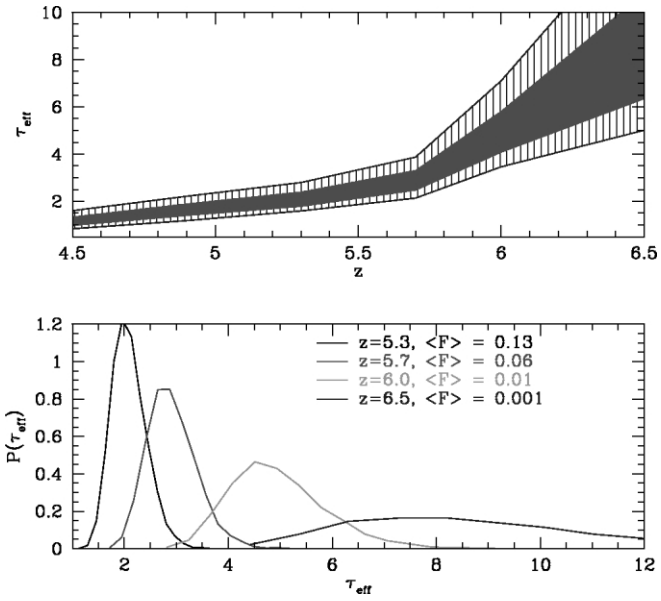

FIG. 3.—Evolution of $\tau_{\rm eff}$ and the expected sight line–to–sigh tline scatter. *Top panel:* 68% and 95% confidence regions for $\tau_{\rm eff}$, smoothed on $L = 40$ Mpc h^{-1}. Notice that the shaded regions become quite broad at large $\tau_{\rm eff}$. We assume $\langle F\rangle = 0.32$, 0.20, 0.13, 0.06, 0.01, and 0.001 at $z = 4.5$, 4.9, 5.3, 5.7, 6.0, and 6.5 respectively. The upper limits on $\tau_{\rm eff}$ at $z = 6.5$ are $\tau_{\rm eff} = 10.8$, 14 (68%, 95% confidence, respectively). *Bottom panel:* Examples of the corresponding PDFs. [*See the electronic edition of the Journal for a color version of this figure.*]

small periodic boxes many times. Figure 1 and equation (3) show that this method must *underestimate* the transmissivity scatter. For instance, Paschos & Norman (2005) use a simulation with $L_{\rm box} = 6.8$ Mpc h^{-1}. Even in the best case extrapolation, we calculate that they underestimate the transmissivity variance on scales $L = 50$ Mpc h^{-1} by a factor of ~2.

Equation (3) does not capture the full story because the flux PDF is actually non-Gaussian. (Note that $\sigma_{\langle F\rangle}/\langle F\rangle \sim 1$ but that $0 < F < 1$.) To reliably calculate confidence intervals, we thus need the full PDF of the smoothed transmission. Because its extrapolation is nontrivial (in contrast to P_F), we calculate the PDF directly from the simulation box. Thus, we effectively smooth on $L = L_{\rm box} = 40$ Mpc h^{-1}, but we still underestimate the width of the PDF because of the large-scale power missing from our box. The bottom panel of Figure 3 shows that the PDF of $\tau_{\rm eff}$ becomes increasingly broad and skewed at high redshift, with a long tail toward high optical depth. This asymmetry implies a bias in measurements of $\tau_{\rm eff}$ from small data samples.

The top panel of Figure 3 shows error bands for the expected sight line–to–sight line scatter in $\tau_{\rm eff}(z)$, adopting a smoothing length of $L = 40$ Mpc h^{-1}. Even for large smoothing scales, the scatter increases rapidly with redshift. We therefore caution against overinterpreting the increasing scatter seen in plots of $\tau_{\rm eff}(z)$ in the literature.

How do our predictions compare with observations? We compare them with recent measurements from Table 5 of Fan et al. (2005), which indicate dispersions of $\tau = (2.1 \pm 0.3, 2.5 \pm 0.5, 2.6 \pm 0.6, 3.2 \pm 0.8, 4.0 \pm 0.8, 7.1 \pm 2.1)$ at $z = (4.90$–$5.15, 5.15$–$5.35, 5.35$–$5.55, 5.55$–$5.75, 5.75$–$5.95, 5.95$–$6.25)$.[7] Interpolating from our results, which assume a slightly different $\tau_{\rm eff}(z)$, we find $\tau = 2.1^{+0.38}_{-0.28}(^{+0.79}_{-0.47})$, $2.5^{+0.46}_{-0.32}(^{+0.94}_{-0.58})$, $2.6^{+0.48}_{-0.33}(^{+0.98}_{-0.61})$, $3.2^{+0.67}_{-0.39}(^{+1.4}_{-0.78})$, $4.0^{+0.99}_{-0.48}(^{+2.0}_{-0.98})$, $7.1^{+3.9}_{-0.60}(^{+7.1}_{-1.9})$, where the intervals indicate 68% (95%) confidence regions. Note that Fan et al. (2005) smoothed over $\Delta z = 0.15$, corresponding to $L = 44$ (56) Mpc h^{-1} at $z = 6$ (5), slightly different than our simulation box ($L_{\rm box} = 40$ Mpc h^{-1}). We conclude that our results are broadly consistent with the measurements of Fan et al. (2005), although we remark that the dispersion is not the ideal statistic to compare with since the PDF of $\tau_{\rm eff}$ is asymmetric. We reiterate that *our calculations assume a uniform radiation field and indicate a scatter that is already comparable to the measured values.*

Furthermore, several systematic effects will tend to *increase* the observed scatter relative to our predictions (see also Tytler et al. 2004). First, as remarked previously, our simulations miss large-scale power. Second, the quasar continua were estimated using a single power law extrapolated from redward of the Lyα forest (e.g., Fan et al. 2005). In reality, quasar continua contain structure and vary significantly between objects (e.g., Bernardi et al. 2003), which may account for some of the apparent transmissivity fluctuations in the data. Next, Lyman limit systems are underproduced in simulations, but they add large-scale power to the transmission (e.g., McDonald et al. 2005). Finally, metal-line absorbers are inevitably present in the observed Lyα forest yet are not included in our calculations. We emphasize that it is important to quantify this systematic scatter, in order to discern the significance of the slight excess scatter in the data.

3.1. *Sight Line–to–Sight Line Scatter in the Lyβ Forest*

What about the transmissivity scatter in the Lyβ forest? To compute that, we must consider fluctuations in the foreground Lyα forest as well. Dijkstra et al. (2004) show that the total power spectrum $P_{F,\,\rm tot}$ is

$$P_{F,\,\rm tot}(k) = P_{F,\,\alpha}(k) + P_{F,\,\beta}(k) + \int \frac{dk'}{2\pi} P_{F,\,\alpha}(k-k')P_{F,\,\beta}(k'). \quad (4)$$

The last term in equation (4) occurs because the total correlation function involves a product, which transforms into a convolution term. Although higher order in the transmissivity fluc-

[7] The dispersions of the last two bins are lower limits, since some lines of sight have complete absorption troughs.

tuations (Dijkstra et al. 2004), this term increases the total variance by ~10%–20% here.

Nonetheless, over an equivalent comoving patch, transmission fluctuations in the Lyβ forest are substantially smaller than in the Lyα forest. We can see this heuristically from the earlier analytic argument by noting that $A_\beta = A_\alpha/6.24$. In practice, this implies fractional fluctuations that are ~2–4 times smaller in the Lyβ forest. From the simulations, over a 50 Mpc h^{-1} interval at $z = 6$ (assuming $\langle F_\alpha \rangle = 0.01$ and hence $\langle F_\beta \rangle = 0.19$ in a clumpy IGM; see Oh & Furlanetto 2005), we obtain $\sigma_{\langle F_{\rm tot}\rangle}/\langle F_{\rm tot}\rangle \sim 0.35$, compared to $\sigma_{\langle F\rangle}/\langle F\rangle = 0.8$ for Lyα fluctuations. If instead $\langle F_\alpha \rangle = 0.001$ at $z = 6$ (and thus $\langle F_\beta \rangle = 0.085$), we obtain $\sigma_{\langle F_{\rm tot}\rangle}/\langle F_{\rm tot}\rangle \sim 0.45$, compared to $\sigma_{\langle F\rangle}/\langle F\rangle \sim 2$ for Lyα fluctuations. Thus, in principle, the Lyβ forest is a more robust indicator of a fluctuating radiation field. Unfortunately, contamination by the Lyγ forest presently limits the Lyβ forest to small number statistics. For instance, Fan et al. (2005) have 97 and 19 measurements (each of size $\Delta z = 0.15$) of the Lyα and Lyβ forests, respectively, spanning $z = 4.8$–6.3 in Lyα and $z = 5.3$–6.3 in Lyβ. The observed Lyβ scatter (their Fig. 3) is also consistent with density fluctuations alone.

4. CONCLUSIONS

We do not mean to imply that the radiation field is indeed uniform at $z \sim 6$. Our intent is only to show that ruling out the *null hypothesis* that the scatter in the high-redshift Lyα forest results solely from density fluctuations requires subtlety. Indeed, we find that density fluctuations alone cause *order unity* transmissivity fluctuations at $z \sim 6$ on scales of $L \sim 50$ Mpc h^{-1}. We therefore caution against attributing the large scatter in $\tau_{\rm eff}$ seen in the spectra of $z \sim 6$ quasars to fluctuations in the ionizing background. In future work, we intend to model the effect of inhomogeneous reionization on the statistics of the Lyα forest, following up on the work of Furlanetto & Oh (2005), and to design statistical measures to discern the presence or absence of these fluctuations.

Finally, we point out that a similar calculation applies to scatter in the transmissivity of the He II Lyα forest near $z \sim 3$. Specifically, we measure the flux power spectrum in the He II Lyα forest assuming $\tau_{\rm eff,\,He\,II} \sim 4$ at $z = 2.9$ (calibrated to the measurements of Smette et al. 2002). The observed scatter is measured in narrow bins with comoving length scales of $L \sim 18$–36 Mpc h^{-1}. At this redshift, we find that is $\sigma_{\langle F,\,\rm He\,II\rangle}/\langle F_{\rm He\,II}\rangle = 1.6$–$1.2$ on these smoothing scales. Again, we caution against interpreting the observed scatter as a signature of fluctuations in the He II ionizing background.

A. L. thanks K. Heitmann and S. Habib for their help with the HPM simulation. We thank L. Hernquist, L. Hui, O. Zahn, and M. Zaldarriaga for stimulating conversations. S. P. O. acknowledges NSF grant AST0407084 for support.

REFERENCES

Becker, R. H., et al. 2001, AJ, 122, 2850
Bernardi, M., et al. 2003, AJ, 125, 32
Croft, R. A. C., et al. 2002, ApJ, 581, 20
Dijkstra, M., Lidz, A., & Hui, L. 2004, ApJ, 605, 7
Eisenstein, D. J., & Hu, W. 1999, ApJ, 511, 5
Fan, X., et al. 2002, AJ, 123, 1247
———. 2005, AJ submitted (astro-ph/0512082)
Furlanetto, S. R., & Oh, S. P. 2005, MNRAS, 363, 1031
Gnedin, N. Y. 2000, ApJ, 535, 530
Gnedin, N. Y., & Hui, L. 1998, MNRAS, 296, 44
Heitmann, K., Ricker, P. M., Warren, M. S., & Habib, S. 2005, ApJS, 160, 28
Hui, L., Gnedin, N. Y., & Zhang, Y., 1997, ApJ, 486, 599
Iliev, I. T., Mellema, G., Pen, U., Merz, H., Shapiro, P. R., & Alvarez, M. A. 2005, MNRAS, submitted (astro-ph/0512187)
Kaiser, N., & Peacock, J. A. 1991, ApJ, 379, 482
Kohler, K., Gnedin, N. Y., & Hamilton, A. J. S. 2005, preprint (astro-ph/0511627)
Lidz, A., Heitmann, K., Hui, L., Habib, S., Rauch, M., & Sargent, W. L. W. 2006, ApJ, 638, 27
Lidz, A., Hui, L., Zaldarriaga, M., & Scoccimarro, R. 2002, ApJ, 579, 491
McDonald, P., et al. 2005, MNRAS, 360, 1471
Miralda-Escudé, J., Cen, R., Ostriker, J. P., & Rauch, M., 1996, ApJ, 471, 582
Miralda-Escudé, J., Haehnelt, M. G., & Rees, M. J. 2000, ApJ, 530, 1
Oh, S. P., & Furlanetto, S. R. 2005, ApJ, 620, L9
Paschos, P., & Norman, M. L. 2005, ApJ, 631, 59
Peacock, J. A., & Dodds, S. J. 1996, MNRAS, 280, L19
Scherrer, R. J., & Weinberg, D. H. 1998, ApJ, 504, 607
Smette, A., et al. 2002, ApJ, 564, 542
Sokasian, A., Abel, T., & Hernquist, L. 2003, MNRAS, 340, 473
Songaila, A., & Cowie, L. 2002, AJ, 123, 2183
Tytler, D., et al. 2004, ApJ, 617, 1
White, R. L., Becker, R. H., Fan, X., & Strauss, M. A. 2003, AJ, 126, 1
———. 2005, AJ, 129, 2102
Wyithe, J. S. B., & Loeb, A. 2005, ApJ, submitted (astro-ph/0508604)